# Nilpotent Singularities and Chaos: Tritrophic Food Chains

Fátima Drubi[a], Santiago Ibáñez[a,*], Paweł Pilarczyk[b]

[a]*Department of Mathematics, University of Oviedo, c/ Federico García Lorca 18, 33007 Oviedo, Spain*
[b]*Faculty of Applied Physics and Mathematics, Gdańsk University of Technology, ul. Gabriela Narutowicza 11/12, 80-233 Gdańsk, Poland*

**Abstract**

Local bifurcation theory is used to prove the existence of chaotic dynamics in two well-known models of tritrophic food chains. To the best of our knowledge, the simplest technique to guarantee the emergence of strange attractors in a given family of vector fields consists of finding a 3-dimensional nilpotent singularity of codimension 3 and verifying some generic algebraic conditions. We provide the essential background regarding this method and describe the main steps to illustrate numerically the chaotic dynamics emerging near these nilpotent singularities. This is a general-purpose method and we hope it can be applied to a huge range of models.

*Keywords:* nilpotent singularities, trophic models, strange attractors.
*2010 MSC:* 58K45, 37D45, 37N25

## 1. Introduction

Mechanisms underlying the genesis of oscillations in predator-prey populations were successfully explained in the celebrated papers [1] and [2]. Since then, the study of ditrophic food chains became one of the major topics in Theoretical Ecology. Working with tritrophic food chains, Hastings and Powel [3] showed that they could exhibit chaotic behavior (see also the earlier reference [4]).

---

*Corresponding author
Email address:* mesa@uniovi.es (Santiago Ibáñez)

7   Subsequent studies [5, 6, 7, 8, 9, 10, 11] or, more recently, [12, 13, 14, 15]), were

8   devoted to describe the dynamics of these models, particularly the mechanisms

9   that lead to the emergence of chaos.

10   In this paper we use a tool, already introduced in [16, 17, 18] and based

11   on local bifurcation theory, to prove the existence of chaotic behavior. Namely,

12   we will explain how some singularities can play a role of organizing centers for

13   chaotic dynamics. The method is applied to two very well-known models of the

14   tritrophic food chain and illustrated with numerical explorations. The steps to

15   apply this technique to other models are also described.

A general tritrophic food chain system is defined by

$$\begin{cases} x' = f_1(x) - g_1(x)y, \\ y' = f_2(y) + g_1(x)y - g_2(y)z, \\ z' = f_3(z) + g_2(y)z. \end{cases} \quad (1)$$

16   This system models the interaction between three different species, namely veg-

17   etation $(x)$, herbivores $(y)$ and predators $(z)$. The functions $f_i$, with $i = 1, 2, 3$,

18   represent the growth rates of vegetation, herbivores and predators, respectively,

19   when the other species are absent. The interaction between different species is

20   also modeled in the system by means of those terms that depend on the functions

21   $g_i$ with $i = 1, 2$. As mentioned in the ecological literature, the most common

22   interactions between consumers and resources are the functional responses of

23   Lotka-Volterra and Holling type II. Both types of consumer-resource interac-

24   tions can be modelled in a single system of differential equations by defining the

25   functions $g_i(u) = \alpha_i u/(1 + k_i u)$, with $\alpha_i > 0$ and $k_i \geq 0$, for $i = 1, 2$. Namely,

26   conditions $k_i = 0$ and $k_i > 0$ correspond to Lotka-Volterra and Holling type II

27   interactions, respectively.

28   We consider here two particular cases for the system in (1):

$$\text{Model A} \quad \begin{cases} x' = a(x - x_0) - \alpha_1 xy, \\ y' = -by + \alpha_1 xy - \alpha_2 yz, \\ z' = -c(z - z_0) + \alpha_2 yz, \end{cases} \quad (2)$$

2

29   where $a$, $b$, $c$, $x_0$ and $z_0$ are positive parameters, and

$$\text{Model B} \quad \begin{cases} x' = rx(1 - px) - \frac{\alpha_1 x}{1 + k_1 y} y, \\ y' = -by + \frac{\alpha_1 x}{1 + k_1 y} y - \alpha_2 yz, \\ z' = -c(z - z_0) + \alpha_2 yz, \end{cases} \qquad (3)$$

30   where $r$, $p$, $b$, $c$, $x_0$ and $z_0$ are positive parameters.

In Model A, it is assumed the possible existence of other consumers affecting the growth of vegetation through the term $x_0$ and also the existence of alternative sources of food available for predators through the term $z_0$. In this case, Lotka-Volterra conditions are considered for all interactions. This model was studied and discussed in [19], providing numerical evidences of chaotic dynamics when

$$a = 1,\ b = 1,\ c = 10,\ \alpha_1 = 0.1,\ \alpha_2 = 0.6,\ x_0 = 1.5,\ z_0 = 0.01.$$

Regarding the intra-specific dynamics, a natural assumption is to consider a logistic law to model the growth of herbivores. This is the case in Model B. In particular, when $p = 0$, Model B corresponds to the case studied in [20], where authors provided numerical evidences of chaotic behavior when

$$r = 1,\ p = 0,\ b = 1,\ c = 10,\ \alpha_1 = 0.2,\ \alpha_2 = 1,\ k_1 = 0.05,\ z_0 = 0.006.$$

31   According to [20, 19], systems (2) and (3) with $p = 0$ model, for example, a
32   classical food web of lynx, hare and vegetation. It should be noted that when
33   $z_0 = 0$ and the Lotka-Volterra interaction between predators and herbivores is
34   replaced by a Holling type II interaction, equations in (3) correspond to the
35   Hastings-Powell model (see [3]).

36   Our main aim in this paper is to show the existence of chaotic dynamics in
37   models A and B by proving that the appropriate singularities are unfolded. In-
38   deed, we demonstrate that both models unfold generically 3-dimensional nilpo-
39   tent singularities. On the other hand, literature provides results establishing
40   that close to these singularities there exist strange attractors (see [16] and also
41   [17, 18]).

Singular perturbation theory has also been successfully applied to explain the emergence of chaotic behavior in tritrophic food chains. For instance, in [9] and [6], it is used to study the existence of chaos in the Rosenzweig–MacArthur (see also [21, 22, 23]). Singular perturbation analysis is also applied to a food chain with four species in [24, 25, 26].

There are numerous models in the literature in which the arguments for the existence of chaotic behavior rest on numerical evidence. However, analytical proofs are considerably less common. To understand the relationship between singularities and homoclinic orbits, as well as their role in the context of Chaos Theory, we must go back to the first demonstrations of the existence of chaotic behavior.

Poincaré [27] was the first to notice the dynamical complexity implied by the existence of a homoclinic orbit associated with a saddle type hyperbolic fixed point of a difeomorphism. By a *homoclinic orbit* we mean the orbit of a homoclinic point, that is, an intersection point between the invariant manifolds of the saddle. Poincaré understood that, if such intersection is transverse, any neighborhood of the primary homoclinic orbit contains an infinite number of secondary ones. Later, Birkhoff [28] proved that in that situation, there also exists an intricate set of periodic orbits with a wide variety of periods. This complicated scenario cried out for a geometric structure that would explain the dynamics as a whole. It was in 1965 that Smale [29] devised his famous horseshoe and placed it in a neighborhood of a transverse homoclinic point. The Lorenz attractor [30] was already known at that time and the notion of chaos was being introduced in the field of dynamical systems. Later, the numerical results of Hénon [31] would come as an example of what was called a strange attractor.

Without going into details, an attractor is called *strange* if it contains a dense orbit with a positive Lyapunov exponent. This last condition is the hallmark of a chaotic system and explains the divergence of orbits within the attractor or, in other words, the high sensitivity of the system to initial conditions, which makes it unpredictable. Despite the impressive numerical examples of Lorenz and Hénon, it still took several years for the first analytical proof of the existence

4

73 of strange attractors to appear.

In 1991, another celebrated article [32] was published, a mathematical masterpiece in which Benedicks and Carleson managed to demonstrate the existence of strange attractors in the Hénon family

$$
\begin{pmatrix} x \\ y \end{pmatrix} \rightarrow \begin{pmatrix} 1 - ax^2 + y \\ bx \end{pmatrix}, \tag{4}
$$

74 where $a, b \in \mathbb{R}$. They considered (4) as a perturbation of a quadratic map re-
75 garding $b$ as a small parameter. The existence of strange attractors holds for a
76 positive measure set of parameter values. At the same time, using the techniques
77 introduced in [32], Mora and Viana [33] proved that in any generic 1-parameter
78 unfolding of a homoclinic tangency for a 2-dimensional diffeomorphism, there
79 exists a positive measure set of parameters for which the diffeomorphism ex-
80 hibits (Hénon-like) strange attractors. Once again, the starting point was to
81 understand these families as unfoldings of a 1-dimensional quadratic map. The
82 results in [33] are essential in our discussion (see also [34]).

83 The next step was to place homoclinic tangency bifurcations for 2-dimensional
84 difeomorphisms in the context of families of 3-dimensional vector fields. Given
85 a 3-dimensional vector field with a saddle type hyperbolic equilibrium point $p$,
86 any orbit $\gamma$ with limit $p$ when $t \rightarrow \pm\infty$ is said *homoclinic*. We say that the
87 homoclinic orbit is *of Shilnikov type* if $p$ is a saddle-focus with eigenvalues $\lambda$
88 and $-\rho \pm \omega i$ satisfying $0 < \rho < \lambda$ . The dynamics in a neighborhood of these
89 homoclinic orbits was first studied by Shilnikov [35]. He proved the existence
90 of infinitely many periodic orbits of saddle type in each neighborhood of the
91 homoclinic orbit. This property should remind us Birkhoff's result for trans-
92 verse homoclinic points in 2-dimensional diffeomorphisms. In fact, it can be
93 proved (see [36, 37]) that the first return map around the homoclinic orbit ex-
94 hibits an infinity of Smale horseshoes. Extended by the flow of the vector field,
95 these horseshoes generate invariant 3-dimensional sets (suspended horseshoes)
96 that accumulate in the homoclinic orbit. Each horseshoe contains an infinite
97 number of transverse homoclinic orbits, where Poincaré's intuition works again.

When the vector field is unfolded to produce a homoclinic bifurcation, these horseshoes are destroyed. The process of creating and destroying horseshoes is accompanied by unfoldings of homoclinic tangencies to hyperbolic periodic points [38, 39] and, therefore, the existence of strange attractors follows from [33] (see also [40, 41, 42]) .

Consequently, there are global configurations, the Shilnikov-type homoclinic orbits, which unfold strange attractors. Since the theory predicts their existence for a positive measure set of parameter values, these strange attractors are observable. Unfortunately, for a given family, Shilnikov homoclinic orbits are not easy to detect, even though there are several results in the literature regarding the emergence of chaos that are based on the numerical location of Shilnikov homoclinic orbits.

Fortunately, it has been proved in [16] that Shilnikov homoclinic orbits, and hence Hénon-like strange attractors, arise in any generic unfolding of a 3-dimensional nilpotent singularity of codimension 3 (see also [17, 43], and [18] for additional technical details). The key argument is the fact that, rescaling variables and parameters, any of such unfoldings can be written as a perturbation of a vector field that exhibits a heteroclinic cycle formed by two saddle-focus equilibria with different stability indexes. Two branches of the 1-dimensional invariant manifolds are coincident and the two-dimensional invariant manifolds intersect transversely. This cycle is a codimension two configuration whose unfolding shows, generically, Shilnikov-type homoclinic bifurcation curves. Therefore, under generic assumptions to be set in Section 2, the existence of nilpotent singularities implies the emergence of chaotic behavior in a given family. In this paper, we show that this method (not related to singular perturbations) can be applied to detect chaos in tritrophic food chains.

Singularities are much more manageable objects than Shilnikov homoclinic orbits. It is a remarkable fact that the steps involved in finding a given singularity and verifying a few generic algebraic conditions become the simplest technique for proving the existence of chaotic dynamics. Applications can be found, for example, in [44, 45, 46, 47, 48, 49].

6

It must be mentioned, however, that the method, although results in proving the existence of Shilnikov homoclinic orbits and thus strange attractors, does not provide us with the (precise) location of neither the strange attractors nor the Shilnikov homoclinic bifurcations in the parameter space. In order to illustrate the chaotic behavior numerically, an alternative method must be used. One possibility is to search for homoclinic bifurcation points by continuation of the periodic orbit emerging from a Hopf bifurcation point. If the periodic orbit disappears in a homoclinic bifurcation, we will see that the period of the orbit tends to infinity. If the homoclinic orbit is of Shilnikov type, we will also see period doubling cascades that precede the formation of the horseshoes, as argued in [39, 50]. As we have already explained, the process of creating or destroying horseshoes is accompanied by the appearance of strange attractors. Ultimately, tracking the attracting periodic orbit in the doubling cascade allows for strange attractors to be located.

**Remark 1.1.** *It must be remarked that three is not the lowest codimension from which it is possible to unfold chaotic behaviors. It is known that there exist Hopf-Zero singularities of codimension two which generically unfold Shilnikov homoclinic orbits. However, part of the genericity conditions depend on the full jet of the singularity and numerical techniques are required for their computation. See [51, 52] and references therein.*

In Section 2, we provide the essential technical background regarding 3-dimensional nilpotent singularities and the generic conditions which are required to guarantee the emergence of strange attractors. Existence and genericity of 3-dimensional nilpotent singularities in models A and B is discussed in Section 3. Moreover, numerical illustrations of dynamics close to nilpotent singularities are given in Section 4. Finally, we discuss in Section 5 the potential applications of our tool, based on local bifurcation theory, to prove the existence of chaotic dynamics.

7

## 2. Nilpotent singularities

Let $X$ be a $C^\infty$ vector field in $\mathbb{R}^3$ with $X(0) = 0$ and $DX(0)$ linearly conjugated to

$$N = \begin{pmatrix} 0 & 1 & 0 \\ 0 & 0 & 1 \\ 0 & 0 & 0 \end{pmatrix}. \tag{5}$$

In appropriate $C^\infty$ coordinates (see [53]), the equations of $X$ can be written as

$$\begin{cases} x_1' = x_2, \\ x_2' = x_3, \\ x_3' = f(x_1, x_2, x_3), \end{cases} \tag{6}$$

with $f(x_1, x_2, x_3) = O(\|(x_1, x_2, x_3)\|^2)$. It is said that $X$ has a *nilpotent singularity of codimension* 3 at 0 if the generic condition

$$d_{11} = \frac{\partial^2 f}{\partial x_1^2}(0) \neq 0 \tag{7}$$

is fulfilled.

According to [53], we can state the result below:

**Lemma 2.1.** *Let $X_\lambda$ be a $C^\infty$ family of 3-dimensional vector fields with $\lambda = (\lambda_1, \lambda_2, \lambda_3) \in \mathbb{R}^3$ such that $X_0$ has a nilpotent singularity of codimension 3 at 0. Under generic assumptions about the derivatives of the family with respect to parameters, and also after changing to new suitable coordinates $\bar{x}$ and parameters $\bar{\lambda}$, the family $X_\lambda$ can be written as*

$$\begin{cases} \bar{x}_1' = \bar{x}_2, \\ \bar{x}_2' = \bar{x}_3, \\ \bar{x}_3' = \bar{\lambda}_1 + \bar{\lambda}_2 \bar{x}_2 + \bar{\lambda}_3 \bar{x}_3 + \bar{x}_1^2 + h(\bar{x}, \bar{\lambda}), \end{cases} \tag{8}$$

*with $\bar{x} = (\bar{x}_1, \bar{x}_2, \bar{x}_3) \in \mathbb{R}^3$, $\bar{\lambda} = (\bar{\lambda}_1, \bar{\lambda}_2, \bar{\lambda}_3) \in \mathbb{R}^3$, $h(\bar{x}, \bar{\lambda}) = O(\|(\bar{x}, \bar{\lambda})\|^2)$ and $h(\bar{x}, \bar{\lambda}) = O(\|(\bar{x}_2, \bar{x}_3)\|)$.*

Genericity in Lemma 2.1 includes the condition in (7), regarding the singularity itself, and a transversality condition involving derivatives of the family

8

with respect to parameters. To be precise, assuming that only the condition in (7) is fulfilled, it was proved (see details in [53] or [46]) that, using appropriate $C^\infty$ coordinates, the family $X_\lambda$ can be written as

$$
\begin{cases}
\bar{x}_1' = \bar{x}_2, \\
\bar{x}_2' = \bar{x}_3, \\
\bar{x}_3' = m_1(\lambda) + m_2(\lambda)\bar{x}_2 + m_3(\lambda)\bar{x}_3 + \bar{x}_1^2 + g(\bar{x}, \lambda),
\end{cases}
\tag{9}
$$

with $g(\bar{x}, \lambda) = O(\|(\bar{x}, \lambda)\|^2)$ and $g(\bar{x}, \lambda) = O(\|(\bar{x}_2, \bar{x}_3)\|)$. The unfolding in (9) is said to be generic if $m(\lambda) = (m_1(\lambda), m_2(\lambda), m_3(\lambda))$ is a local diffeomorphism at the origin or, in other words, if the generic condition below

$$
\Delta = \det(Dm(0)) \neq 0
\tag{10}
$$

is satisfied. With this assumption we can introduce new parameters

$$
(\bar{\lambda}_1, \bar{\lambda}_2, \bar{\lambda}_3) = (m_1(\lambda), m_2(\lambda), m_3(\lambda))
$$

162  to obtain (8).

163  For the sake of completeness, we provide simple formulas to check the generic

164  assumptions. Let us write $X_\lambda(x) = (X^{(1)}(x, \lambda), X^{(2)}(x, \lambda), X^{(3)}(x, \lambda))$ and as-

165  sume that $DX_0(0) = N$. We consider the notation

$$
\gamma_i^{(k)} = \frac{\partial X^{(k)}}{\partial \lambda_i}(0, 0), \qquad \Lambda_{ij}^{(k)} = \frac{\partial^2 X^{(k)}}{\partial \lambda_i \partial x_j}(0, 0),
$$

$$
A_{ii}^{(k)} = \frac{1}{2}\frac{\partial^2 X^{(k)}}{\partial x_i^2}(0, 0), \qquad A_{ij}^{(k)} = \frac{\partial^2 X^{(k)}}{\partial x_i \partial x_j}(0, 0) \quad (\text{when } i \neq j),
$$

for $i, j, k = 1, 2, 3$. It follows from [53] that

$$
d_{11} = 2A_{11}^{(3)}.
\tag{11}
$$

The coefficient $A_{11}^{(3)}$ remains unchanged after reducing the system to the normal form. Therefore, we assume that, up to a change of coordinates, $A_{11}^{(3)} = 1$. Using the formulas provided in [46], we easily obtain

$$
\Delta = \begin{vmatrix}
\gamma_1^{(3)} & \gamma_2^{(3)} & \gamma_3^{(3)} \\
P_1^* + \sum_{k=1}^2 P_k \gamma_1^{(k)} & P_2^* + \sum_{k=1}^2 P_k \gamma_2^{(k)} & P_3^* + \sum_{k=1}^2 P_k \gamma_3^{(k)} \\
Q_1^* + \sum_{k=1}^2 Q_k \gamma_1^{(k)} & Q_2^* + \sum_{k=1}^2 Q_k \gamma_2^{(k)} & Q_3^* + \sum_{k=1}^2 Q_k \gamma_3^{(k)}
\end{vmatrix}
\tag{12}
$$

9

for all $i = 1, 2, 3$, with

$$
\begin{aligned}
P_i^* &= \Lambda_{i2}^{(3)} + \Lambda_{i1}^{(2)} - \frac{1}{2}\left(A_{12}^{(3)} + 2A_{11}^{(2)}\right)\Lambda_{i1}^{(3)}, \\
P_1 &= -\left(2A_{22}^{(3)} + A_{12}^{(2)} - \frac{1}{2}A_{12}^{(3)}\left(A_{12}^{(3)} + 2A_{11}^{(2)}\right)\right), \\
P_2 &= -\left(A_{23}^{(3)} + A_{13}^{(2)} - \frac{1}{2}A_{13}^{(3)}\left(A_{12}^{(3)} + 2A_{11}^{(2)}\right)\right), \\
Q_i^* &= \Lambda_{i3}^{(3)} + \Lambda_{i2}^{(2)} + \Lambda_{i1}^{(1)} - \frac{1}{2}\left(A_{13}^{(3)} + A_{12}^{(2)} + 2A_{11}^{(1)}\right)\Lambda_{i1}^{(3)}, \\
Q_1 &= -\left(A_{23}^{(3)} + 2A_{22}^{(2)} + A_{12}^{(1)} - \frac{1}{2}A_{12}^{(3)}\left(A_{13}^{(3)} + A_{12}^{(2)} + 2A_{11}^{(1)}\right)\right), \\
Q_2 &= -\left(2A_{33}^{(3)} + A_{23}^{(2)} + A_{13}^{(1)} - \frac{1}{2}A_{13}^{(3)}\left(A_{13}^{(3)} + A_{12}^{(2)} + 2A_{11}^{(1)}\right)\right).
\end{aligned}
$$

**Remark 2.2.** *The additional condition*

$$
d_{12} = \frac{\partial^2 g}{\partial x_1 \partial x_2}(0) \neq 0 \tag{13}
$$

*is also required to prove the existence of strange attractors (see [18]). It follows from [46] that*

$$
d_{12} = A_{12}^{(3)} + 2A_{11}^{(2)}. \tag{14}
$$

Several aspects of the dynamics arising in unfoldings of the 3-dimensional nilpotent singularity of codimension 3 has been studied in ([53, 17, 43, 16, 18]). In [16, 18], it was proved that any unfolding satisfying the generic conditions (7), (10) and (13) displays Shilnikov homoclinic orbits and hence, as argued in the introduction, strange attractors.

**Remark 2.3.** *As the simple formulas provided in (11), (12) and (14) are effortless computable, in this paper we describe an easy-to-check method to prove the existence of chaotic behavior in a given model. This will become a very helpful technique for further applications in the detection of chaos.*

## 3. Chaos in tritrophic food chain models

In this section we prove that models in (2) and (3) are indeed generic unfoldings of 3-dimensional nilpotent singularities and, hence, they exhibit strange

10

179    attractors. Note that, in both cases, some coefficients can be normalized. There-

180    fore, in what follows, we assume that $a = 1$ and $r = 1$ in (2) and (3), respectively.

181    *3.1. Nilpotent singularities in Model A*

182        The study of equilibria of model in (2) provides the below result regarding

183    the existence of a nilpotent singularity.

**Proposition 3.1.** *Assume that $\alpha_2 \neq \alpha_1$, $\alpha_2 \neq \alpha_1 c$ and $c \neq 1$ in (2). When*
$(x_0, z_0, b) = (\hat{x}_0, \hat{z}_0, \hat{b})$ *with*

$$\hat{x}_0 = \frac{(\alpha_2 - \alpha_1 c)^3}{2\alpha_1^2(\alpha_2 - \alpha_1)^2(c - 1)}, \qquad \hat{z}_0 = \frac{(\alpha_2 - \alpha_1 c)^3}{2\alpha_2^2(\alpha_2 - \alpha_1)^2 c(c - 1)},$$

*and*

$$\hat{b} = \frac{(\alpha_2 - \alpha_1 c)^2}{2\alpha_1\alpha_2(c - 1)},$$

*system (2) has an equilibrium point at $(\hat{x}, \hat{y}, \hat{z})$ with*

$$\hat{x} = \frac{(\alpha_2 - \alpha_1 c)^2}{2\alpha_1^2(\alpha_2 - \alpha_1)(c - 1)}, \quad \hat{y} = \frac{c - 1}{\alpha_2 - \alpha_1}, \quad \hat{z} = \frac{(\alpha_2 - \alpha_1 c)^2}{2\alpha_2^2(\alpha_2 - \alpha_1)(c - 1)},$$

184    *where the Jacobian matrix is linearly conjugated to $N$ as given in (5).*

*Proof.* From the first and third equation in (2) it follows that an equilibrium
$(\hat{x}, \hat{y}, \hat{z})$ must satisfy that

$$\hat{x} = \frac{x_0}{1 - \alpha_1\hat{y}} \qquad \text{and} \qquad \hat{z} = \frac{cz_0}{c - \alpha_2\hat{y}}. \tag{15}$$

Replacing $x$ and $z$ by $\hat{x}$ and $\hat{z}$, respectively, in the second equation of system
(2), we obtain that either

$$b = \alpha_1\hat{x} - \alpha_2\hat{z} \tag{16}$$

185    or $y = 0$. It is here assumed that (16) is fulfilled because otherwise we obtain a

186    singularity at $(x_0, 0, z_0)$ and it can be checked that is not nilpotent.

To characterize the nilpotent singularities we need to compute the linear
part of (2) at $(\hat{x}, \hat{y}, \hat{z})$. The Jacobian matrix is given by

$$\begin{pmatrix} 1 - \alpha_1\hat{y} & -\alpha_1\hat{x} & 0 \\ \alpha_1\hat{y} & 0 & -\alpha_2\hat{y} \\ 0 & \alpha_2\hat{z} & -c + \alpha_2\hat{y} \end{pmatrix}$$

11

and the characteristic polynomial is

$$c_0 + c_1\lambda + c_2\lambda^2 - \lambda^3,$$

with

$$c_0 = \hat{y}(\alpha_1^2(-c + \alpha_2\hat{y})\hat{x} + \alpha_2^2(1 - \alpha_1\hat{y})\hat{z}),$$
$$c_1 = -((1 - \alpha_1\hat{y})(-c + \alpha_2\hat{y}) + \alpha_1^2\hat{x}\hat{y} + \alpha_2^2\hat{y}\hat{z}),$$
$$c_2 = 1 - c + \hat{y}(\alpha_2 - \alpha_1).$$

The equilibrium at $(\hat{x}, \hat{y}, \hat{z})$ is a nilpotent singularity if $c_0 = c_1 = c_2 = 0$. Assuming that $c_2 = 0$, we easily obtain

$$\hat{y} = \frac{c - 1}{\alpha_2 - \alpha_1}.$$

Therefore, substituting $\hat{y}$ in (15), we get

$$\hat{x} = \frac{x_0(\alpha_2 - \alpha_1)}{\alpha_2 - \alpha_1 c} \qquad \hat{z} = \frac{c z_0(\alpha_2 - \alpha_1)}{\alpha_2 - \alpha_1 c}. \qquad (17)$$

Substituting $\hat{x}$, $\hat{y}$ y $\hat{z}$ in the equations $c_0 = 0$ and $c_1 = 0$, and assuming that $c \neq 1$, we obtain the system below:

$$\begin{cases} \alpha_1^2 x_0 + \alpha_2^2 c z_0 & = & \frac{(\alpha_2 - \alpha_1 c)^3}{(c-1)(\alpha_2 - \alpha_1)^2} \\ \alpha_1^2 x_0 - \alpha_2^2 c z_0 & = & 0, \end{cases} \qquad (18)$$

which is linear in the unknown parameters $x_0$ and $z_0$. The solutions of this systems are

$$x_0 = \frac{(\alpha_2 - \alpha_1 c)^3}{2\alpha_1^2(\alpha_2 - \alpha_1)^2(c - 1)} \qquad z_0 = \frac{(\alpha_2 - \alpha_1 c)^3}{2\alpha_2^2(\alpha_2 - \alpha_1)^2(c - 1)c}.$$

Hence, substituting $x_0$ and $z_0$ in (17)

$$\hat{x} = \frac{(\alpha_2 - \alpha_1 c)^2}{2\alpha_1^2(\alpha_2 - \alpha_1)(c - 1)} \qquad \hat{z} = \frac{(\alpha_2 - \alpha_1 c)^2}{2\alpha_2^2(\alpha_2 - \alpha_1)(c - 1)}$$

and then substituting $\hat{x}$ and $\hat{z}$ in (16) we get

$$\hat{b} = \frac{(\alpha_2 - \alpha_1 c)^2}{2\alpha_1\alpha_2(c - 1)}.$$

It easily follows that the rank of the Jacobian matrix is equal to 2 and hence it is linearly conjugated to $N$. $\qquad\square$

12

To check all the generic conditions given in Section 2, we consider $x_0$, $z_0$ and $b$ as bifurcation parameters and fix all the others at the values provided by a bifurcation point to a nilpotent singularity. After an appropriate $C^\infty$ change of coordinates, the equations of Model A can be written with a canonical linear part as in system (2.1). Therefore, from formulas (11) and (14), it follows that

$$d_{11} = \frac{2\,\alpha_2\,(c\,\alpha_1 - \alpha_2)\,(c-1)}{\alpha_1 - \alpha_2} \tag{19}$$

and

$$d_{12} = \frac{\alpha_1\,(c-3) + \alpha_2\,(3\,c-1)}{(c\,\alpha_1 - \alpha_2)\,(c-1)}. \tag{20}$$

Moreover, using (12), we get

$$\Delta = \frac{c\,\alpha_1^2\,\alpha_2^2\,(c\,\alpha_1 - \alpha_2)\,(c-1)^3}{(\alpha_1 - \alpha_2)^3}. \tag{21}$$

It easily follows that the values $\hat{x}_0$, $\hat{z}_0$ and $\hat{b}$ and also $\hat{x}$, $\hat{y}$ and $\hat{z}$ (as given in Proposition 3.1) are all positive if and only if $c > 1$ and $\alpha_2 > \alpha_1 c$. Such conditions also imply that $d_{11} \neq 0$ and $\Delta \neq 0$. Moreover, $d_{12} \neq 0$ under the additional condition

$$\alpha_1\,(c-3) + \alpha_2\,(3\,c-1) \neq 0. \tag{22}$$

Thus, as the conditions given in (7), (10) and (13) fulfill, Model A unfolds generically 3-dimensional nilpotent singularities and exhibits strange attractors.

**Remark 3.2.** *Formulas given in (19), (20) and (21) are not unique but depend on the $C^\infty$ change of coordinates. Nevertheless, after any change of variables, it can be easily check that $d_{11} \neq 0$ and $\Delta \neq 0$ when $c > 1$ and $\alpha_2 > \alpha_1 c$, as well as $d_{12} \neq 0$ under the additional condition (22).*

*3.2. Nilpotent singularities in Model B*

The study of equilibria of model in (3) provides the below result regarding the existence of a nilpotent singularity.

**Proposition 3.3.** *Let*

$$\Phi_1 = p + k_1(2ps - 1),$$

$$\Phi_2 = 2(ps-1)^2(1+k_1s)^2\alpha_2 - s^2\Phi_1^3.$$

*When* $(z_0, b, c, \alpha_1) = (\hat{z}_0, \hat{b}, \hat{c}, \hat{\alpha}_1)$ *with*

$$\hat{z}_0 = \frac{-s^5\Phi_1^7}{4(1+k_1s)^3(ps-1)^2\alpha_2^2\Phi_2},$$

$$\hat{b} = \frac{-s^2\Phi_1^2\left(2(ps-1)(1+k_1s)^2\alpha_2 + s\Phi_1^2\right)}{4(1+k_1s)^3(ps-1)^2\alpha_2},$$

$$\hat{c} = \frac{\Phi_2}{s(1+k_1s)\Phi_1^2},$$

$$\hat{\alpha}_1 = \frac{-s\Phi_1^2}{2(ps-1)},$$

*system (3) has an equilibrium point at* $(\hat{x}, \hat{y}, \hat{z})$ *with*

$$\hat{x} = s, \quad \hat{y} = \frac{2(1+k_1s)(ps-1)^2}{s(p+k_1(2ps-1))^2}, \quad \hat{z} = \frac{s^3(p+k_1(2ps-1))^4}{4(1+k_1s)^3(ps-1)^2\alpha_2^2}.$$

*Whenever* $\hat{x}, \hat{y}, \hat{z} > 0$, *the Jacobian matrix at the equilibrium point is conjugated to* $N$ *as given in (5).*

*Proof.* From the first and third equation in (3), it follows that an equilibrium $(\hat{x}, \hat{y}, \hat{z})$ satisfies that

$$\hat{y} = -\frac{(1 + k_1\hat{x})(p\hat{x} - 1)}{\alpha_1} \qquad \text{and} \qquad \hat{z} = \frac{cz_0}{c - \alpha_2\hat{y}}.$$

Replacing $z$ by $\hat{z}$ in the second equation of system (3), we also obtain that either

$$\hat{y} = \frac{c\left((b + z_0\alpha_2)(1 + k_1\hat{x}) - \alpha_1\hat{x}\right)}{(b(1 + k_1\hat{x}) - \alpha_1\hat{x})\alpha_2} \tag{23}$$

or $\hat{y} = 0$. It is here assumed that (23) is fulfilled because it can be checked that otherwise the singularities are not nilpotent. Therefore, it is also assumed that $\hat{x} \neq \frac{1}{k_1}$ and $\hat{x} \neq \frac{1}{p}$.

Hence, we get that

$$-\frac{(1 + k_1\hat{x})(p\hat{x} - 1)}{\alpha_1} = \frac{c\left((b + z_0\alpha_2)(1 + k_1\hat{x}) - \alpha_1\hat{x}\right)}{(b(1 + k_1\hat{x}) - \alpha_1\hat{x})\alpha_2}.$$

14

213 Solving the above equation to find $c$, we obtain

$$\hat{c} \equiv \hat{c}(\hat{x}, p, k_1, \alpha_1, \alpha_2, z_0) = -\frac{(1 + k_1\hat{x})(p\hat{x} - 1)(b(1 + k_1\hat{x}) - \alpha_1\hat{x})\alpha_2}{\alpha_1\left((b + z_0\alpha_2)(1 + k_1\hat{x}) - \alpha_1\hat{x}\right)}.$$

The characteristic polynomial of the Jacobian matrix at $(\hat{x}, \hat{y}, \hat{z})$ is

$$c_0 + c_1\lambda + c_2\lambda^2 - \lambda^3,$$

214 where $c_0$, $c_1$ and $c_2$ are functions of $(\hat{x}, p, b, z_0, \alpha_1, \alpha_2, k_1)$.

The equilibrium at $(\hat{x}, \hat{y}, \hat{z})$ is a nilpotent singularity if $c_0 = c_1 = c_2 = 0$. Assuming that $c_2 = 0$, we easily obtain $\hat{b} \equiv \hat{b}(\hat{x}, p, k_1, \alpha_1, \alpha_2, z_0)$. Substituting $b$ by $\hat{b}$ in $c_0 = 0$, we obtain

$$\hat{z}_0 \equiv \hat{z}_0(\hat{x}, p, k_1, \alpha_1, \alpha_2) = \frac{\alpha_1^3\hat{x}^2(p + k_1(-1 + 2p\hat{x}))}{\alpha_2^2(1 + k_1\hat{x})^3 g(\hat{x}, p, k_1, \alpha_1, \alpha_2)}.$$

with $g(\hat{x}, p, k_1, \alpha_1, \alpha_2) = k_1^2\hat{x}^2(p\hat{x} - 1)\alpha_2 + p\hat{x}(\alpha_1 + \alpha_2) - \alpha_2 + k_1\hat{x}[(2p\hat{x} - 1)\alpha_1 + 2(p\hat{x} - 1)\alpha_2]$. Substituting $b$ by $\hat{b}$ and $z_0$ by $\hat{z}_0$ in $c_1 = 0$, we get

$$\hat{\alpha}_1 \equiv \hat{\alpha}_1(\hat{x}, p, k_1) = \frac{-\hat{x}(p + k_1(2p\hat{x} - 1))^2}{2(p\hat{x} - 1)}.$$

215 Substituting $\alpha_1$ by $\hat{\alpha}_1$ in $\hat{z}_0$, the formula of $\hat{z}_0$ can be written as a function
216 of $(\hat{x}, p, k_1, \alpha_2)$. Similarly, substituting $\alpha_1$ by $\hat{\alpha}_1$ and $z_0$ by $\hat{z}_0$ in $\hat{b}$, we obtain a
217 formula for $\hat{b}$ that depends only on $(\hat{x}, p, k_1, \alpha_2)$. In addition, we can also write
218 $\hat{c}$ as a function of $(\hat{x}, p, k_1, \alpha_2)$. Finally, we replace $\hat{x}$ by an extra parameter $s$
219 to get all the formulas provided in the statement.

220 It easily follows that, when $\hat{x}, \hat{y}, \hat{z} > 0$, the rank of the Jacobian matrix is
221 equal to 2 and hence it is linearly conjugated to $N$. □

222 To prove that Model B is a generic unfolding of the 3-dimensional nilpo-
223 tent singularity characterized in Proposition 3.3, the generic conditions given in
224 Section 2 have to be checked as well. In this case, we consider $z_0$, $b$ and $c$ as
225 bifurcation parameters and fix the others at the values provided by a bifurca-
226 tion point to a nilpotent singularity. Therefore, from formulas (11) and (14), it
227 follows that

$$d_{11} = \frac{2\alpha_2(ps - 1)(k_1^3 s^2\Psi_1 + k_1^2 s^2\Psi_2 + 2k_1 s\Psi_3 - 2\alpha_2(ps - 1))}{(1 + k_1 s)^2(p + k_1(2ps - 1))}, \quad (24)$$

$$d_{12} = \frac{2\alpha_2(\Psi_4 + p^2\Psi_5 + k_1^2 s\Psi_6 + 2k_1 s\Psi_7)}{s(1 + k_1 s)(p + k_1(2ps - 1))^2 d_{11}}. \quad (25)$$

15

Using (12), it follows

$$\Delta = \frac{s\,\alpha_2{}^2(ps-1)^2\,\Psi_8\,\left(\Psi_9 + k_1{}^2 s^2\,\Psi_{10} + k_1 s\,\Psi_{11}\right)}{(1+k_1 s)^3\,(p+k_1\,(2ps-1))^2}. \tag{26}$$

In the above expressions,

$$
\begin{aligned}
\Psi_1 &= 1 - 5ps + 6p^2 s^2, \\
\Psi_2 &= 7p^2 s + 2\alpha_2 - p(3 + 2s\alpha_2), \\
\Psi_3 &= p^2 s + 2\alpha_2 - 2ps\alpha_2, \\
\Psi_4 &= p^3 s^2 + 2k_1^3 ps^3(2ps - 1) - 6\alpha_2 + 12ps\alpha_2, \\
\Psi_5 &= s - 6s^2\alpha_2, \\
\Psi_6 &= 1 - 6s\alpha_2 - 6p^2 s^2(s\alpha_2 - 2) + ps(12s\alpha_2 - 7), \\
\Psi_7 &= p^3 s^2 - 6\alpha_2 + 3p^2 s(1 - 2s\alpha_2) + p(12s\alpha_2 - 1), \\
\Psi_8 &= -p + k_1 - 6\,p\,s\,k_1 + 4\,p^2\,s^2\,k_1, \\
\Psi_9 &= p^3\,s^2 + s^2\,(2\,p\,s - 1)^3\,k_1{}^3 - 2\,\alpha_2 + 4\,p\,s\,\alpha_2 - 2\,p^2\,s^2\,\alpha_2 \\
\Psi_{10} &= 12\,p^3\,s^2 - 2\,\alpha_2 - 2\,p^2\,s\,(6 + s\,\alpha_2) + p\,(3 + 4\,s\,\alpha_2), \\
\Psi_{11} &= 6\,p^3\,s^2 - 4\,\alpha_2 + 8\,p\,s\,\alpha_2 - p^2\,s\,(3 + 4\,s\,\alpha_2).
\end{aligned}
$$

In this case, it is not easy to state simple conditions to guarantee that (24), (25) and (26) do not vanish and also that coordinates and parameters are all of them positive at the bifurcation point. In the next section, we find positive parameter values $s$, $p$, $\alpha_2$ and $k_1$ for which $\hat{z}_0$, $\hat{b}$, $\hat{c}$ and $\hat{\alpha}_1$ and also $\hat{x}$, $\hat{y}$ and $\hat{z}$ (as given in Proposition 3.3) are all positive. Moreover, we check that generic conditions (7), (10) and (13) are fulfilled. Therefore, it follows that Model B unfolds generically 3-dimensional nilpotent singularities and, hence, exhibits strange attractors.

**Remark 3.4.** *Computations are straightforward through formulas (11), (12) and (14). Nevertheless, most of them are lengthy and we have used the Symbolic Math Toolbox in Matlab® to carry out many of them.*

16

## 4. Numerical simulations

In this section, we study numerically the bifurcation diagram of both models A in (2) and B in (3). For the purpose of simulations, the equations are solved numerically in Matlab$^{\circledR}$, using the MatCont package [54] for numerical bifurcation analysis. We also show the emergence of chaotic dynamics near the nilpotent singularity generically unfolded in these models. In section 2, the well-known techniques to ensure that a given family of differential equations exhibits chaotic dynamics were reduced to a small number of algebraic calculations. Thus, the necessary conditions become easy to check for any family. Nevertheless, although the theoretical results guarantee that generic unfoldings of 3-dimensional nilpotent singularities include strange attractors, this technique is not a tool in itself to find numerically strange attractors and extra work has to be done to locate a region in the parameter space where chaotic behavior emerges. As we believe that formulae in section 2 will be useful to study the emergence of chaotic dynamics in many other models, we describe here the main steps to show numerically the chaotic dynamics near the nilpotent singularity in our models.

### 4.1. Model A

We work with parameters values close to those considered in [19] and, therefore, in what follows in this section we set

$$c = 3, \qquad \alpha_1 = \frac{3}{25}, \qquad \text{and} \quad \alpha_2 = \frac{4}{5}.$$

Using formulae provided in Proposition 3.1, we get

$$\hat{x}_0 = \frac{33275}{10404}, \qquad \hat{z}_0 = \frac{1331}{55488}, \qquad \hat{b} = \frac{121}{240},$$

and hence the equilibrium point is at

$$\hat{x} = \frac{3025}{612}, \qquad \hat{y} = \frac{50}{17}, \qquad \hat{z} = \frac{121}{1088}.$$

Substituting these parameter values in formulae (19), (20) and (21), we easily obtain

$$d_{11} = \frac{176}{85}, \qquad d_{12} = \frac{-80}{11}, \qquad \text{and} \quad \Delta = \frac{38016}{122825}.$$

17

258    Therefore, Model A is a generic 3-parametric unfolding of a 3-dimensional

259    nilpotent singularity. The parameters of the unfolding are $x_0$, $z_0$ and $b$ and a

260    nilpotent singularity appears at $(\hat{x}, \hat{y}, \hat{z})$ when $x_0 = \hat{x}_0$, $z_0 = \hat{z}_0$ and $b = \hat{b}$.

To study the bifurcation diagram near the nilpotent singularity, we consider
$(\mu_1, \mu_2, \mu_3)$ as new parameters and work with the family below

$$
\begin{cases}
x' = x - \hat{x}_0 - \mu_1 - \alpha_1 xy, \\
y' = -(\hat{b} + \mu_2)y + \alpha_1 xy - \alpha_2 yz, \\
z' = -c(z - \hat{z}_0 - \mu_3) + \alpha_2 yz.
\end{cases}
\tag{27}
$$

261    The theoretical results in section 3 guarantee that family (27) includes

262    strange attractors. To illustrate this result we set $\mu_3 = 0.01$ and study the

263    bifurcation diagram of (27) in the $(\mu_1, \mu_2)$-parameter plane. A Hopf bifurcation

264    curve and a saddle-node bifurcation curve are detected near the 3-dimensional

265    nilpotent singularity (see Figure 1(a)). Moreover, by continuation in the param-

266    eter $\mu_2$ (see Figure 1(b)) of the periodic orbit emerging from the Hopf bifurcation

267    detected when $\mu_1 = 0.6182493995438856$, a period doubling bifurcation is de-

268    tected (see the blue curve in Figure 1(c)). An additional period doubling is

269    shown in Figure 1(c). In Figure 1(d) we provide a bifurcation diagram of period

270    doubling cascades.

271    The existence of period doubling cascades is itself an evidence of chaos,

272    but because we have put the emphasis in the existence of Shilnikov homoclinic

273    orbits, we show an example in Figure 2. We plot, as approximations of the

274    homoclinic connection, the orbit which is computed at the end point of the

275    numerical continuation of the 1-periodic orbit (see the blue curve in Figure

276    1(c)). Note that there exists an infinite sequence of saddle-node bifurcations

277    and the period of the orbit tends to infinity. As period increases, parameter $\mu_2$

278    tends to a certain limit which can be approached by the value of $\mu_2$ at the end

279    point of the continuation, namely, 0.0784693743654685.

280    It is known that, moving parameters to break the homoclinic orbit, one

281    should be able to detect the existence of strange attractors. In this case, we

282    perturb the vector field by changing slightly the value of the $\mu_2$ (see Figure 3).
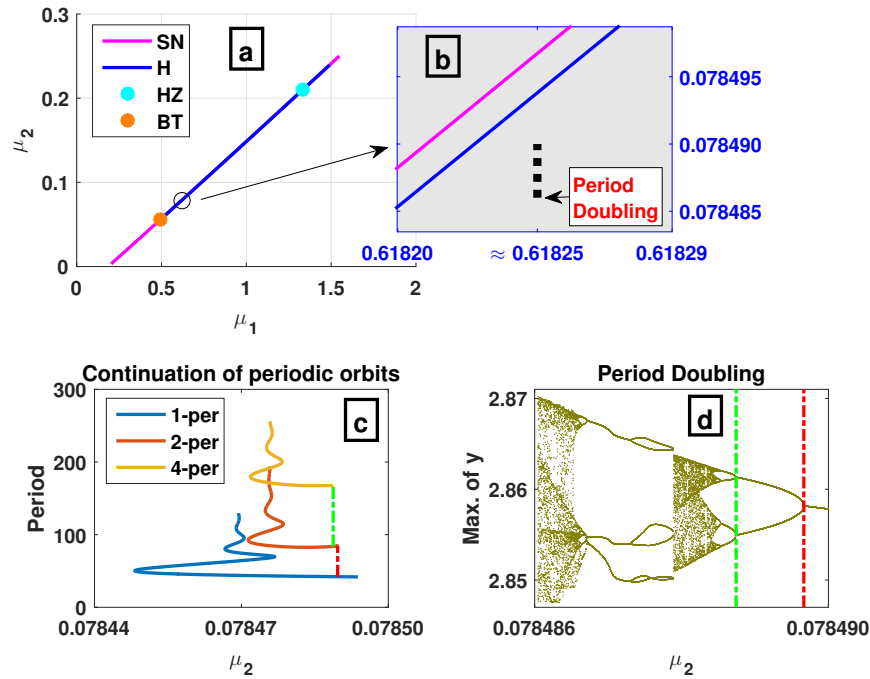
18

Figure 1: Model A: Numerical bifurcation analysis of the 3-parametric family (27) near the 3-dimensional nilpotent singularity. (a) A bifurcation diagram is shown in the $(\mu_1, \mu_2)$-parameter plane, with fixed parameter $\mu_3 = 0.01$. A saddle-node bifurcation curve (SN) and a Hopf bifurcation curve (H) as well as a Hopf-Zero bifurcation point (HZ) and a Bogdanov-Takens bifurcation point (BT) are found. (b) A region in the $(\mu_1, \mu_2)$-parameter plane is enlarged to show the segment where the cascades of period doubling bifurcations are detected. Along such segment $\mu_1 = 0.6182493995438856$ is fixed. (c) Two period doubling bifurcations are shown. (d) Cascades of period doubling bifurcations. The red and green dashed lines are in correspondence with those in (c).

The graphs of the solutions are included to show that the oscillations have a regular phase rhythm while the abundance peaks in each cycle are unpredictable. This features of uniform phase and chaotic amplitudes are exhibited by many biological systems ([20, 19]).
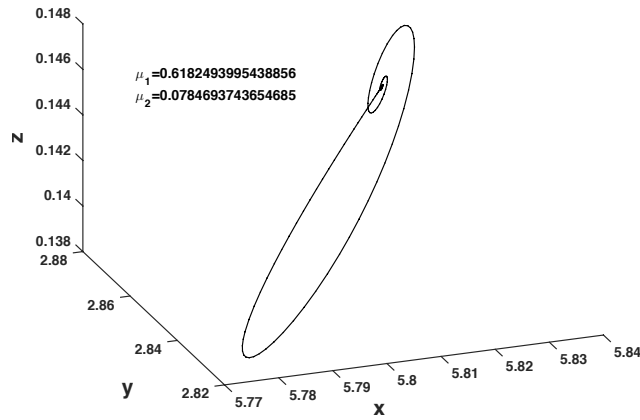
19

Figure 2: Model A: Shilnikov homoclinic orbit. The parameters $\mu_1$ and $\mu_3$ are set as in Figure 1(c). The value of $\mu_2$ is 0.0784693743654685, which corresponds to the value at which the period of the 1-periodic orbit tends to infinity. For that value, the 1-periodic orbit is close enough to a homoclinic orbit.
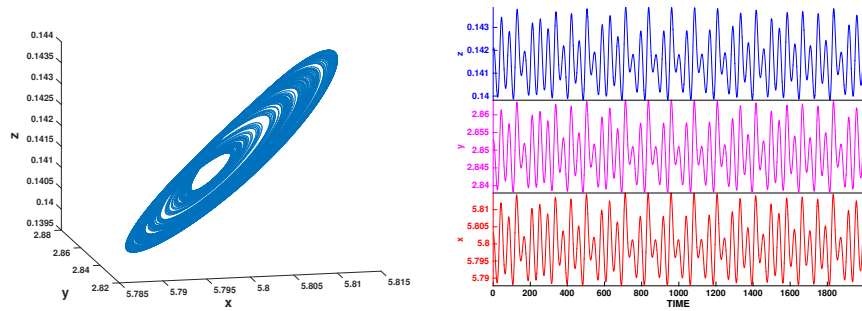


Figure 3: Model A: A strange attractor (left) and the solutions along the strange attractor (right). When the Shilnikov homoclinic orbit is broken, strange attractors can arise. The parameters $\mu_1$ and $\mu_3$ are set as in Figure 1(c) and $\mu_2 = 0.078487896$. The initial point in the plotted orbit is $(x_i, y_i, z_i) = (5.803149567, 2.852761453, 0.142024188)$. This strange attractor was detected exploring the cascade of period doubling bifurcations. The Maximal Lyapunov Exponent is close to 0.01.

20

### 4.2. Model B

We work with parameters values close to those considered in [20] and, therefore, in what follows in this section we set

$$p = 0, \qquad \alpha_2 = \frac{38}{45}, \qquad \text{and} \quad k_1 = \frac{7}{20}.$$

Using formulae provided in Proposition 3.3 with $s = 11$, we get

$$\hat{z}_0 = 0.070896246, \qquad \hat{b} = 1.4762613, \qquad \hat{c} = 6.8725611, \qquad \hat{\alpha}_1 = 0.673750,$$

and hence the equilibrium point is at

$$\hat{x} = 11, \qquad \hat{y} = 7.1985158, \qquad \hat{z} = 0.061379431.$$

Substituting these parameter values in formulae (24), (25) and (26), we easily obtain

$$d_{11} = 9.2137978, \qquad d_{12} = -3.3049085, \qquad \text{and} \quad \Delta = -8.8232932.$$

Therefore, Model B is a generic 3-parametric unfolding of a 3-dimensional nilpotent singularity. The parameters of the unfolding are $z_0$, $b$ and $c$ and a nilpotent singularity appears at $(\hat{x}, \hat{y}, \hat{z})$ when $z_0 = \hat{z}_0$, $b = \hat{b}$ and $c = \hat{c}$.

To study the bifurcation diagram near the nilpotent singularity, we consider $(\mu_1, \mu_2, \mu_3)$ as new parameters and work with the family below

$$\begin{cases} x' = x(1 - px) - \frac{\hat{\alpha}_1 x}{1 + k_1 y} y, \\ y' = -(\hat{b} + \mu_2)y + \frac{\hat{\alpha}_1 x}{1 + k_1 y} y - \alpha_2 yz, \\ z' = -(\hat{c} + \mu_3)(z - \hat{z}_0 - \mu_1) + \alpha_2 yz. \end{cases} \tag{28}$$

The theoretical results in section 3 guarantee that family (28) exhibits strange attractors. To illustrate numerically the chaotic behavior in this family, we set $\mu_3 = 0.005$ and study the bifurcation diagram of (28) in the $(\mu_1, \mu_2)$-parameter plane. Working with MatCont we obtain the results given in Figure 4. The explanation of the different panels is identical to the case of Model A and we do not repeat it here. Only mention that now the cascades of period doublings
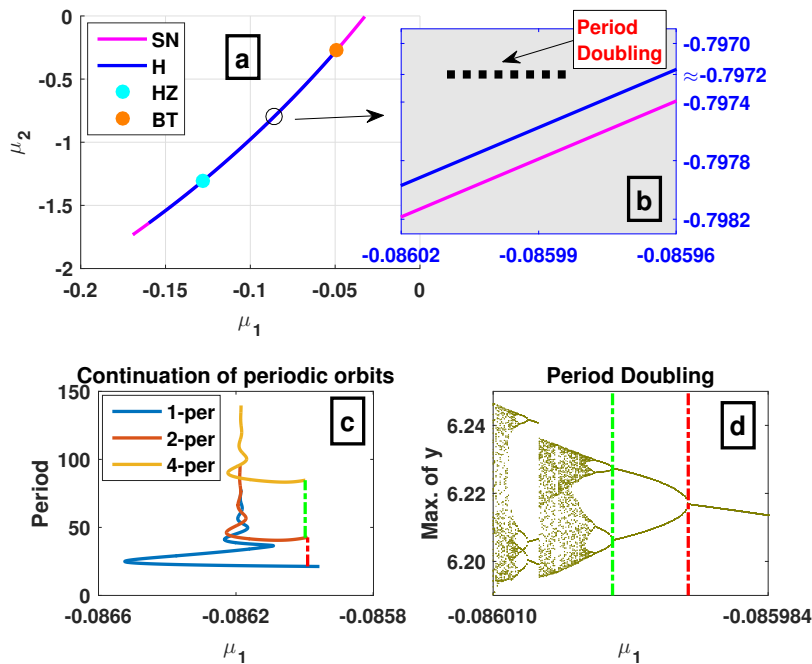
21

Figure 4: Model B: Numerical bifurcation analysis of the 3-parametric family (28) near the 3-dimensional nilpotent singularity. (a) A bifurcation diagram is shown in the $(\mu_1, \mu_2)$-parameter plane, with fixed parameter $\mu_3 = 0.005$. A saddle-node bifurcation curve (SN) and a Hopf bifurcation curve (H) as well as a Hopf-Zero bifurcation point (HZ) and a Bogdanov-Takens bifurcation point (BT) are found. (b) A region in the $(\mu_1, \mu_2)$-parameter plane is enlarged to show the segment where the cascades of period doubling bifurcations are detected. Along such segment $\mu_2 = -0.797211509659839$ is fixed. (c) Two period doubling bifurcations are shown. (d) Cascades of period doubling bifurcations. The red and green dashed lines are in correspondence with those in (c).

are detected fixing $\mu_2 = -0.797211509659839$ and considering $\mu_1$ as the continuation parameter.

We show an example of Shilnikov homoclinic orbit in Figure 5. Namely, we plot the orbit which is computed at the end point of the numerical continuation of the 1-periodic orbit (see blue curve in Figure 4(c)). As period tends to infinity, parameter $\mu_2$ tends to a certain limit which can be approached by the value of $\mu_1$ at the end point of the continuation, namely, $-0.0861858348181701$.
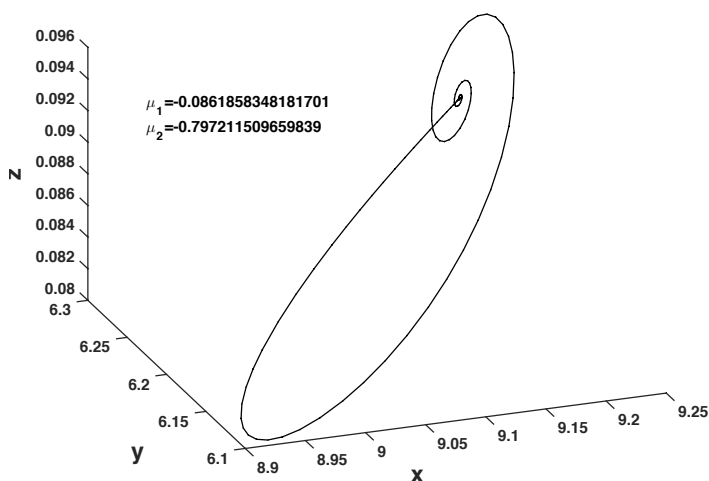
22

Figure 5: Model B: Shilnikov homoclinic orbit. The parameters $\mu_2$ and $\mu_3$ are set as in Figure 4(c). The value of $\mu_1$ is $-0.0861858348181701$, which corresponds to the value at which the period of the 1-periodic orbit tends to infinity. For that value, the 1-periodic orbit is close enough to a homoclinic orbit.

Finally, we perturb the vector field by changing slightly the value of the $\mu_1$ to get an example of strange attractor (see Figure 6). As in case of Model A, the graphs of the solutions are included to show the uniform phase and the chaotic amplitudes, features exhibited by many biological systems ([20, 19]).

## 5. Conclusions

In this paper, we provide an easy-to-check method, based on local bifurcation theory, to prove the existence of chaotic dynamics in a given model. The generic conditions which are required to guarantee the emergence of strange attractors in a generic unfolding of the 3-dimensional nilpotent singularity are reduced to simple formulas in section 2 (see (11), (12) and (14)). Therefore, this technique becomes very helpful for further applications in the detection of chaos. In particular, we apply this method to prove that two different tritrophic chain models
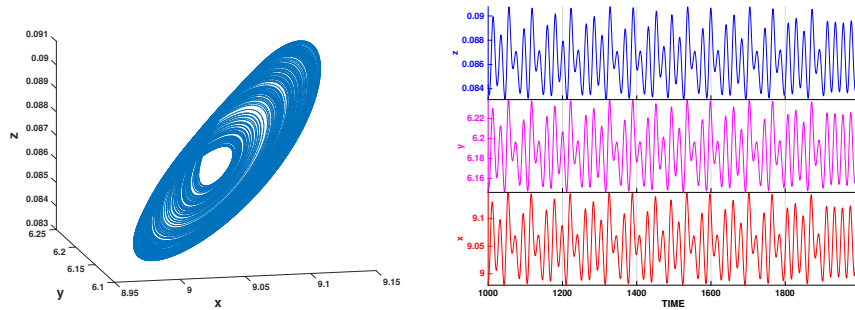
23

Figure 6: Model B: A strange attractor (left) and the solutions along the strange attractor (right). The parameters $\mu_2$ and $\mu_3$ are set as in Figure 4(c) and $\mu_1 = -0.086005637$. The initial point is $(x_i, y_i, z_i) = (9.1412254, 6.2329186, 0.089506456)$ and the chaotic orbit are detected exploring the cascade of period doubling bifurcations. The Maximal Lyapunov Exponent is close to 0.02.

are indeed generic unfoldings of 3-dimensional nilpotent singularities and hence they exhibit strange attractors (see section 3).

For completeness, in section 4, we numerically illustrate the existence of strange attractors in the two tritrophic chain models considered and explain the steps taken. Shortly, for any given model we first consider a point in the parameter space that satisfies the generic conditions. This means that the model is a generic 3-parametric unfolding of a 3-dimensional singularity. Second, we study the bifurcation diagram near the nilpotent singularity to detect a Hopf bifurcation curve. Third, using numerical techniques for continuation of periodic orbits, we are able to find a cascade of period doubling bifurcations and hence strange attractors. Moreover, continuation also allows to allocate parameter values for which the systems exhibits Shilnikov homoclinic orbits.

**Acknowledgements**

24

## References

[1] A. J. Lotka, The elements of physical biology., XXX + 460 p. Baltimore, Williams & Wilkins Co.; London, Baillière, Tindall & Cox (1925). (1925).

[2] V. Volterra, Variazioni e fluttuazioni del numero d'individui in specie animali conviventi., Mem. Accad. naz. Lincei, Cl. Sci. fis. mat. nat. (6) 2 (1927) 31–113.

[3] A. Hastings, T. Powell, Chaos in a 3-species food-chain, Ecology 72 (3) (1991) 896–903. doi:10.2307/1940591.

[4] P. Hogeweg, B. Hesper, Interactive instruction on pouplation interactions, Comput. Biol. Med. 8 (4) (1978) 319–327. doi:10.1016/0010-4825(78)90032-X.

[5] M. P. Boer, B. W. Kooi, S. A. L. M. Kooijman, Homoclinic and heteroclinic orbits to a cycle in a tri-trophic food chain, J. Math. Biol. 39 (1) (1999) 19–38. doi:10.1007/s002850050161.

[6] O. De Feo, S. Rinaldi, Singular homoclinic bifurcations in tritrophic food chains, Math. Biosci. 148 (1) (1998) 7–20. doi:10.1016/S0025-5564(97)10001-3.

[7] A. Klebanoff, A. Hastings, Chaos in 3-species food-chain, J. Math. Biol. 32 (5) (1994) 427–451. doi:10.1007/BF00160167.

[8] Y. A. Kuznetsov, O. De Feo, S. Rinaldi, Belyakov homoclinic bifurcations in a tritrophic food chain model, SIAM J. Appl. Math. 62 (2) (2001) 462–487. doi:10.1137/S0036139900378542.

[9] Y. A. Kuznetsov, S. Rinaldi, Remarks on food chain dynamics, Math. Biosci. 134 (1) (1996) 1–33. doi:10.1016/0025-5564(95)00104-2.

[10] K. McCann, A. Hastings, Re-evaluating the omnivory-stability relationship in food webs, Proceedings: Biological Sciences 264 (1385) (1997) 1249–1254. doi:10.1098/rspb.1997.0172.

25

[11] K. McCann, P. Yozdis, Bifurcation structure of a three-species food-chain model, Theor. Popul. Biol 48 (2) (1995) 93–125. `doi:10.1006/tpbi.1995.1023`.

[12] R. K. Upadhyay, R. K. Naji, Dynamics of a three species food chain model with crowley-martin type functional response, Chaos, Solitons & Fractals 42 (3) (2009) 1337–1346. `doi:10.1016/j.chaos.2009.03.020`.

[13] B. Sahoo, S. Poria, The chaos and control of a food chain model supplying additional food to top-predator, Chaos, Solitons & Fractals 58 (2014) 52–64. `doi:10.1016/j.chaos.2013.11.008`.

[14] M. Saifuddin, S. Samanta, S. Biswas, J. Chattopadhyay, An eco-epidemiological model with different competition coefficients and strong-Allee in the prey, Internat. J. Bifur. Chaos Appl. Sci. Engrg. 27 (8) (2017) 1730027, 23. `doi:10.1142/S0218127417300270`.

[15] P. Panday, N. Pal, S. Samanta, J. Chattopadhyay, Stability and bifurcation analysis of a three-species food chain model with fear, Internat. J. Bifur. Chaos Appl. Sci. Engrg. 28 (1) (2018) 1850009, 20. `doi:10.1142/S0218127418500098`.

[16] S. Ibáñez, J. A. Rodríguez, Shil'nikov configurations in any generic unfolding of the nilpotent singularity of codimension three on $\mathbb{R}^3$, J. Differential Equations 208 (1) (2005) 147–175. `doi:10.1016/j.jde.2003.08.006`.

[17] F. Dumortier, S. Ibáñez, H. Kokubu, New aspects in the unfolding of the nilpotent singularity of codimension three, Dyn. Syst. 16 (1) (2001) 63–95. `doi:10.1080/02681110010017417`.

[18] P. G. Barrientos, S. Ibáñez, J. A. Rodríguez, Heteroclinic cycles arising in generic unfoldings of nilpotent singularities, J. Dynam. Differential Equations 23 (4) (2011) 999–1028. `doi:10.1007/s10884-011-9230-5`.

26

[19] L. Stone, D. He, Chaotic oscillations and cycles in multi-trophic ecological systems, J. Theoret. Biol. 248 (2) (2007) 382–390. `doi:10.1016/j.jtbi.2007.05.023`.

[20] B. Blasius, A. Huppert, L. Stone, Complex dynamics and phase synchronization in spatially extended ecological systems, Nature 399 (6734) (1999) 354–359. `doi:10.1038/20676`.

[21] B. Deng, G. Hines, Food chain chaos due to Shilnikov's orbit, Chaos 12 (3) (2002) 533–538. `doi:10.1063/1.1482255`.

[22] B. Deng, G. Hines, Food chain chaos due to transcritical point, Chaos 13 (2) (2003) 578–585. `doi:10.1063/1.1576531`.

[23] B. Deng, Food chain chaos with canard explosion, Chaos 14 (4) (2004) 1083–1092. `doi:10.1063/1.1814191`.

[24] B. Bockelman, B. Deng, E. Green, G. Hines, L. Lippitt, J. Sherman, Chaotic coexistence in a top-predator mediated competitive exclusive web, J. Dynam. Differential Equations 16 (4) (2004) 1061–1092. `doi:10.1007/s10884-004-7833-9`.

[25] B. Bockelman, B. Deng, E. Green, G. Hines, L. Lippitt, J. Sherman, Erratum to: "Chaotic coexistence in a top-predator mediated competitive exclusive web" [J. Dynam. Differential Equations 16 (2004), no. 4, 1061–1092], J. Dynam. Differential Equations 17 (1) (2005) 217. `doi:10.1007/s10884-005-4560-9`.

[26] B. B., B. D., Food web chaos without subchain oscillators, Internat. J. Bifur. Chaos Appl. Sci. Engrg. 15 (11) (2005) 3481–3492. `doi:10.1142/S0218127405014179`.

[27] H. Poincaré, Sur une forme nouvelle des équations du problème des trois corps, Acta Math. 21 (1) (1897) 83–97. `doi:10.1007/BF02417977`.

[28] G. D. Birkhoff, Nouvelles recherches sur les systèmes dynamiques, Memoriae Pont. Acad. Sci. Novi Lyncaei 1 (1935) 85–216.

[29] S. Smale, Differentiable dynamical systems, Bull. Amer. Math. Soc. 73 (1967) 747–817. `doi:10.1090/S0002-9904-1967-11798-1`.

[30] E. N. Lorenz, Deterministic nonperiodic flow, J. Atmospheric Sci. 20 (2) (1963) 130–141. `doi:10.1175/1520-0469(1963)020<0130:DNF>2.0.CO; 2`.

[31] M. Hénon, A two-dimensional mapping with a strange attractor, Comm. Math. Phys. 50 (1) (1976) 69–77.
URL `http://projecteuclid.org/euclid.cmp/1103900150`

[32] M. Benedicks, L. Carleson, The dynamics of the Hénon map, Ann. of Math. 133 (1) (1991) 73–169. `doi:10.2307/2944326`.

[33] L. Mora, M. Viana, Abundance of strange attractors, Acta Math. 171 (1) (1993) 1–71. `doi:10.1007/BF02392766`.

[34] C. Bonatti, L. J. Díaz, M. Viana, Dynamics beyond uniform hyperbolicity, Vol. 102 of Encyclopaedia of Mathematical Sciences, Springer-Verlag, Berlin, 2005.

[35] L. P. Šil'nikov, A case of the existence of a denumerable set of periodic motions, Dokl. Akad. Nauk SSSR 160 (1965) 558–561.

[36] L. P. Shil'nikov, A contribution to the problem of the structure of an extended neighborhood of a rough equilibrium state of saddle-focus type, Math. USSR, Sb. 10 (1970) 91–102.

[37] C. Tresser, About some theorems by L. P. Sil'nikov, Ann. Inst. H. Poincaré Phys. Théor. 40 (4) (1984) 441–461.

[38] L. J. Díaz, V. Horita, I. Rios, M. Sambarino, Destroying horseshoes via heterodimensional cycles: generating bifurcations inside homoclinic classes,

28

436    Ergodic Theory Dynam. Systems 29 (2) (2009) 433–474. `doi:10.1017/`
437    `S0143385708080346`.

438 [39] J. Palis, F. Takens, Hyperbolicity and sensitive chaotic dynamics at homo-
439    clinic bifurcations, Vol. 35 of Cambridge Studies in Advanced Mathematics,
440    Cambridge University Press, Cambridge, 1993.

441 [40] A. J. Homburg, Periodic attractors, strange attractors and hyperbolic dy-
442    namics near homoclinic orbits to saddle-focus equilibria, Nonlinearity 15 (4)
443    (2002) 1029–1050. `doi:10.1088/0951-7715/15/4/304`.

444 [41] A. Pumariño, J. A. Rodríguez, Coexistence and persistence of strange at-
445    tractors, Vol. 1658 of Lect. Notes Math., Springer-Verlag, Berlin, 1997.
446    `doi:10.1007/BFb0093337`.

447 [42] A. Pumariño, J. A. Rodríguez, Coexistence and persistence of infinitely
448    many strange attractors, Ergodic Theory Dynam. Systems 21 (5) (2001)
449    1511–1523. `doi:10.1017/S0143385701001730`.

450 [43] F. Dumortier, S. Ibáñez, H. Kokubu, Cocoon bifurcation in three-
451    dimensional reversible vector fields, Nonlinearity 19 (2) (2006) 305–328.
452    `doi:10.1088/0951-7715/19/2/004`.

453 [44] A. Algaba, M. Merino, E. Freire, E. Gamero, A. J. Rodríguez-Luis, Some
454    results on Chua's equation near a triple-zero linear degeneracy, Internat.
455    J. Bifur. Chaos Appl. Sci. Engrg. 13 (3) (2003) 583–608. `doi:10.1142/`
456    `S0218127403006741`.

457 [45] S. A. Campbell, Y. Yuan, Zero singularities of codimension two and three
458    in delay differential equations, Nonlinearity 21 (11) (2008) 2671–2691. `doi:`
459    `10.1088/0951-7715/21/11/010`.

460 [46] F. Drubi, S. Ibáñez, J. A. Rodríguez, Coupling leads to chaos, J. Differential
461    Equations 239 (2) (2007) 371–385. `doi:10.1016/j.jde.2007.05.024`.

29

[47] E. Freire, E. Gamero, A. J. Rodríguez-Luis, A. Algaba, A note on the triple-zero linear degeneracy: normal forms, dynamical and bifurcation behaviors of an unfolding, Internat. J. Bifur. Chaos Appl. Sci. Engrg. 12 (12) (2002) 2799–2820. `doi:10.1142/S0218127402006175`.

[48] F. Drubi, S. Ibáñez, J. A. Rodríguez, Singularities and chaos in coupled systems, Bull. Belg. Math. Soc. Simon Stevin 15 (5, Dynamics in perturbations) (2008) 797–808. `doi:10.36045/bbms/1228486408`.

[49] J. Sieber, B. Krauskopf, Bifurcation analysis of an inverted pendulum with delayed feedback control near a triple-zero eigenvalue singularity, Nonlinearity 17 (1) (2004) 85–103. `doi:10.1088/0951-7715/17/1/006`.

[50] J. A. Yorke, K. T. Alligood, Period doubling cascades of attractors: a prerequisite for horseshoes, Comm. Math. Phys. 101 (3) (1985) 305–321. URL `http://projecteuclid.org/euclid.cmp/1104114178`

[51] I. Baldomá, S. Ibáñez, T. M. Seara, Hopf-Zero singularities truly unfold chaos, Commun. Nonlinear Sci. Numer. Simul. 84 (2020) 105162. `doi:10.1016/j.cnsns.2019.105162`.

[52] F. Dumortier, S. Ibáñez, H. Kokubu, C. Simó, About the unfolding of a Hopf-zero singularity, Discrete Contin. Dyn. Syst. 33 (10) (2013) 4435–4471. `doi:10.3934/dcds.2013.33.4435`.

[53] F. Dumortier, S. Ibáñez, Nilpotent singularities in generic 4-parameter families of 3-dimensional vector fields, J. Differential Equations 127 (2) (1996) 590–647. `doi:10.1006/jdeq.1996.0085`.

[54] A. Dhooge, W. Govaerts, Y. A. Kuznetsov, H. G. E. Meijer, B. Sautois, New features of the software MatCont for bifurcation analysis of dynamical systems, Math. Comput. Model. Dyn. Syst. 14 (2) (2008) 147–175. `doi:10.1080/13873950701742754`.